Journal of Applied Physics

Quantum efficiency of InGaN–GaN multi-quantum well solar cells: Experimental characterization and modeling

Cite as: J. Appl. Phys. **131**, 224501 (2022); https://doi.org/10.1063/5.0076833
Submitted: 28 October 2021 • Accepted: 19 May 2022 • Published Online: 08 June 2022

Alessandro Caria, Marco Nicoletto, Carlo De Santi, et al.

Journal of Applied Physics ARTICLE scitation.org/journal/jap

Quantum efficiency of InGaN–GaN multi-quantum well solar cells: Experimental characterization and modeling

Cite as: J. Appl. Phys. **131**, 224501 (2022); doi: 10.1063/5.0076833
Submitted: 28 October 2021 · Accepted: 19 May 2022 ·
Published Online: 8 June 2022

Alessandro Caria,[1,a)] Marco Nicoletto,[1] Carlo De Santi,[1] Matteo Buffolo,[1] Xuanqi Huang,[2] Houqiang Fu,[3] Hong Chen,[2] Yuji Zhao,[2,4] Gaudenzio Meneghesso,[1] Enrico Zanoni,[1] and Matteo Meneghini[1]

AFFILIATIONS

[1]Department of Information Engineering, University of Padova, Via G. Gradenigo 6B, Padova, Italy
[2]School of Electrical, Computer, and Energy Engineering, Arizona State University, Tempe, Arizona 85287, USA
[3]Department of Electrical and Computer Engineering, Iowa State University, Ames, Iowa 50011, USA
[4]Department of Electrical and Computer Engineering, Rice University, Houston, Texas 77005, USA

Note: This paper is part of the Special Topic on Wide Bandgap Semiconductor Materials and Devices.
[a)]**Author to whom correspondence should be addressed:** alessandro.caria@dei.unipd.it

ABSTRACT

InGaN-based multi-quantum well (MQW) solar cells are promising devices for photovoltaics (e.g., for tandem solar cells and concentrator systems), space applications, and wireless power transfer. In order to improve the efficiency of these devices, the factors limiting their efficiency and stability must be investigated in detail. Due to the complexity of a MQW structure, compared with a simple pn junction, modeling the spectral response of these solar cells is not straightforward, and *ad hoc* methodologies must be implemented. In this paper, we propose a model, based on material parameters and closed-formula equations, that describes the shape of the quantum efficiency of InGaN/GaN MQW solar cells, by taking into account the layer thickness, the temperature dependence of the absorption coefficient, and quantum confinement effects. We demonstrate (i) that the proposed model can effectively reproduce the spectral response of the cells; in addition, (ii) we prove that the bulk p-GaN layer absorbs radiation, but the carriers photogenerated in this region do not significantly contribute to device current. Finally, we show that (iii) by increasing the temperature, there is a redshift of the absorption edge due to bandgap narrowing, which can be described by Varshni law and is taken into account by the model, and a lowering in the extraction efficiency due to the increase in recombination (mostly Shockley–Read–Hall) inside the quantum wells, which is also visible by decreasing light intensity.

INTRODUCTION

InGaN–GaN multi-quantum well (MQW) solar cells have a good absorption capacity in the blue and near UV regions. Solar radiation in this range is not efficiently collected by standard semiconductor materials. Consequently, InGaN-based cells can be integrated into multijunction (MJ) solar cells, and this will help increase the efficiency of MJ cells from the current record ~47%[1] to beyond 50%. Further applications of InGaN/GaN MQW cells include silicon-GaN tandem solar cells[2,3] and concentrator systems.[4–6] Moreover, owing to their reliability and strength in harsh environments,[7] InGaN–GaN multiple quantum well devices are also suitable for applications like wireless power transfer[8] and use in the space environment.[9]

To push the development of these devices, it is fundamental to understand the factors that limit their efficiency. Modeling the efficiency of MQW solar cells is not straightforward due to the presence of many semiconductor layers with different absorption coefficients, the presence of barriers for carrier transport, and the existence of quantum effects.[10,11] In this paper, we present an approach to this problem, by developing a model, based on physical considerations, which can be numerically solved to describe the wavelength dependence of quantum efficiency, by taking into

account the thickness and the absorption coefficient of the constituting layers of the device and the related quantum processes.

EXPERIMENTAL DETAILS

The study was carried out on GaN–InGaN–GaN MQW solar cells with a AlGaN electron-blocking layer (EBL) grown on a c-plane sapphire. This EBL is introduced to ease hole extraction; in fact, the EBL reduces the electron–hole recombination at the p-side by blocking the overflowing electrons.[12] The wafers have a 2-μm n-GaN (Si: 3×10^{18} cm^{-3}), 30 pairs of $In_{0.15}Ga_{0.85}N$–GaN (3–7 nm) multiple quantum wells, a 5- nm p-$Al_{0.15}Ga_{0.85}N$ (Mg: 2×10^{19} cm^{-3}) electron-blocking layer, a (Mg: 2×10^{19} cm^{-3}) layer, and a 10 nm p+-GaN (Mg: $>2\times10^{19}$ cm^{-3}) layer. The top layer is made of a 120- nm semi-transparent indium–tin–oxide (ITO) layer with Ti/Pt/Au metal contact, whereas the n-side contact is made of Ti/Al/Ni/Au. 1A, 2A, and 2B variants were analyzed, which had different p-GaN thicknesses of 100, 50, and 150 nm, respectively. The device structures are schematized in Fig. 1(b). More details on the structures can be found in Ref. 12.

A characterization of the external quantum efficiency was carried out by means of a 300 W Xenon arc lamp, whose output was fed into a 1/8- m grating monochromator (full width at half maximum 13.7 nm). The light was focused into an optical fiber, then filtered by reflective neutral density filters up to ND2, and focused on the sample. The experimental setup is schematized in Fig. 1(a). By measuring the optical power with a power meter, it was possible to calculate the external quantum efficiency (EQE) of the sample as the ratio between the number of collected carriers under short-circuit conditions over the number of photons arriving on the device. Reflectivity measurements, made with LOANA instrument by pv-tools GmbH, are reported in Fig. S1 in the supplementary material.

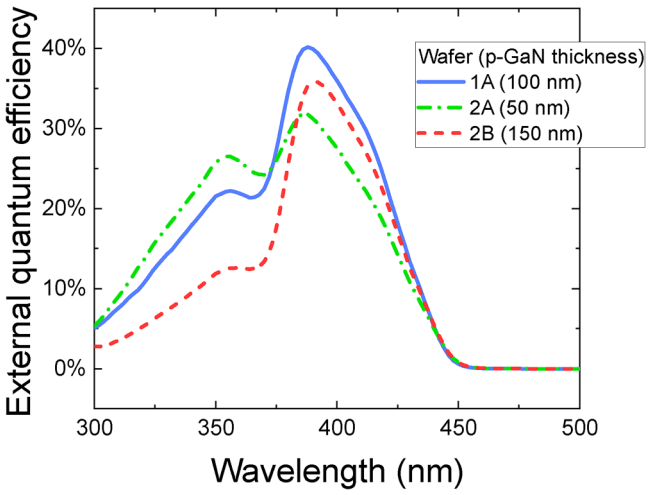

FIG. 2. External quantum efficiency of different samples measured at 35 °C baseplate temperature.

EXPERIMENTAL MEASUREMENTS

A first characterization was made by evaluating the EQE of different samples at 35 °C. The results are shown in Fig. 2. As can be noticed, the shape of the spectral response is significantly different from that of a simple pn-junction solar cell. All the structures have an EQE peak in the region 380–390 nm and a secondary peak in the region around 350 nm. The EQE reaches a maximum of around 40% for the 1A structure, which features the 100 nm p-GaN. The absorption edge starts around 450 nm for all the structures, with minimum differences, possibly due to slight indium fluctuations between the wafers.

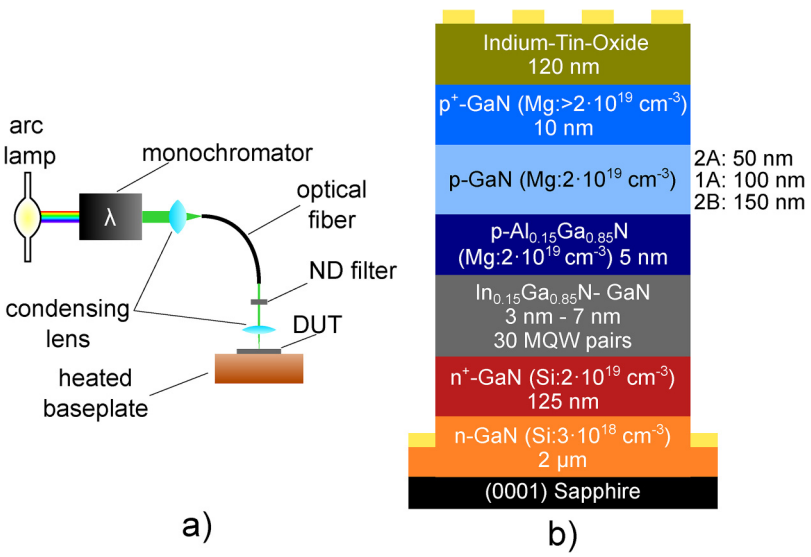

FIG. 1. Schematic of the experimental setup (a) and of the devices under analysis (b).

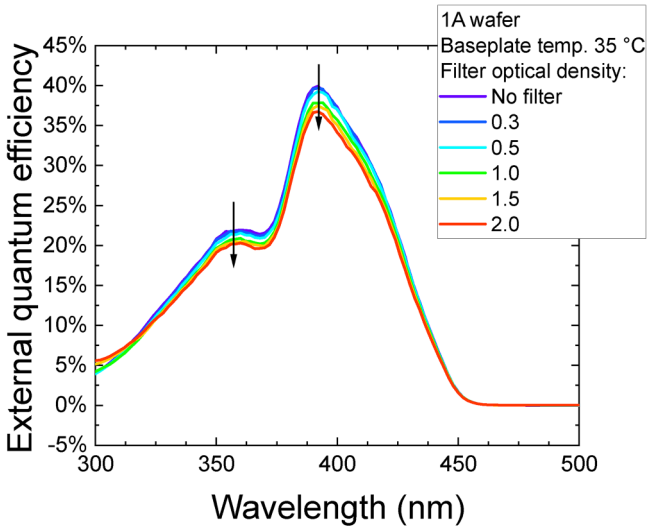

FIG. 3. External quantum efficiency of the 1A sample measured at 35 °C baseplate temperature at different light intensities.

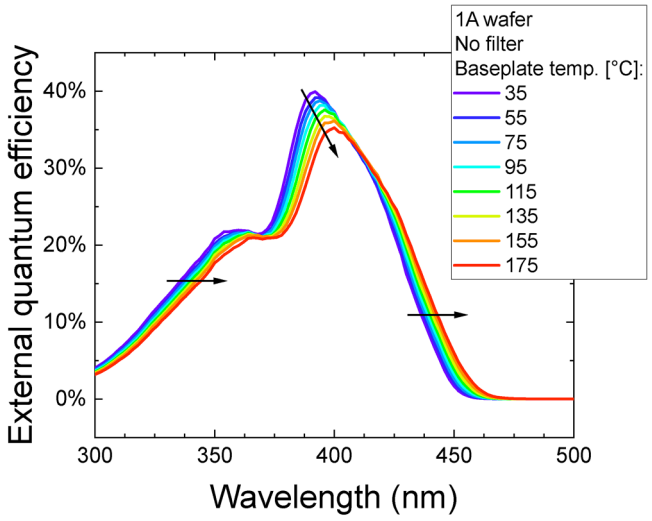

FIG. 4. External quantum efficiency of the 1A sample measured at various baseplate temperatures.

We then illuminated the samples by using the neutral density filters to evaluate the effect of different light intensities on the samples. In Fig. 3, the EQE of the 1A sample is reported, whereas the EQE of the other samples are reported in Figs. S2 and S3 in the supplementary material. As it is possible to see, by decreasing the light intensity of a factor up to 100 (corresponding to a ND2 filter), there is a slight decrease in the EQE, whereas no variation is seen in the absorption edge. The lowering in the EQE with decreasing light intensity is possibly related to a decrease in extraction efficiency from the quantum wells due to a relative increase in Shockley–Read–Hall (SRH) non-radiative recombination: the decrease in light intensity lowers the generation rate, and, therefore, a higher fraction of the photogenerated carrier incurs non-radiative recombination instead of escaping the quantum wells, thus lowering the photocurrent signal and the EQE.[13]

We measured the EQE at the maximum intensity by varying the baseplate temperature from 35 to 175 °C in 20 °C steps. The behavior of the 1A sample is reported in Fig. 4. By increasing the temperature, it is possible to see a redshift of both the main and the secondary peak due to the bandgap narrowing effect. The main edge shift was fitted by the Varshni law,

$$E_g(T) = E_g(0) - \frac{\delta T^2}{\gamma + T}, \tag{1}$$

obtaining $\delta = (6.6 \pm 4.4) \times 10^{-4}$ eV/K, $\gamma = (755 \pm 949)$ K, and $E_g(0) = (2.84 \pm 0.01)$ eV for the 1A device. Due to the lack of data at lower temperatures, the fit quality for the parameters A and B is relatively low, but the found values have a good agreement with the literature, in particular, the $E_g(0)$ value for $In_{0.15}Ga_{0.85}N$.[14,15]

Another side effect of the temperature increase is the lowering in the main peak, which can be ascribed to the same SRH recombination processes that caused the lowering in the EQE with a decreasing temperature, since SRH recombination rate A is proportional to

$$A \propto \frac{1}{\tau_{SRH}} \propto \left[1 + \cosh\left(\frac{\Delta E_T}{k_B T}\right)\right]^{-1}, \tag{2}$$

where τ_{SRH} is the SRH lifetime, k_B is the Boltzmann constant, T is the temperature, and $\Delta E_T = E_T - E_{F_i}$ is the energy difference between the trap level and the intrinsic Fermi level.[16] Thus, by increasing the temperature, the SRH rate also increases, leading to a decrease in the EQE.

The energy of the deep level involved in this process was calculated by fitting the external quantum efficiency maximum of the 1A device with respect to the baseplate temperature with Eq. (2) (see Fig. 5), obtaining an energy of $\Delta E_T = (65 \pm 16)$ meV. Such energy equals a trap level with $E_V +$ or $E_C - (1.3 - 1.5)$ eV inside the quantum wells, which is attributed to several defects in gallium nitride,[17] such as carbon interstitials[18–20] or gallium vacancies and their complexes.[21–24]

ANALYSIS AND MODELING

To better understand the shape of the quantum efficiency curve and, thus, to improve device capability to convert light radiation into electric power, we developed a physical model of the photocurrent based on several simple assumptions:

1. Light enters on the device p-side and is partly reflected according to reflectivity measurements.

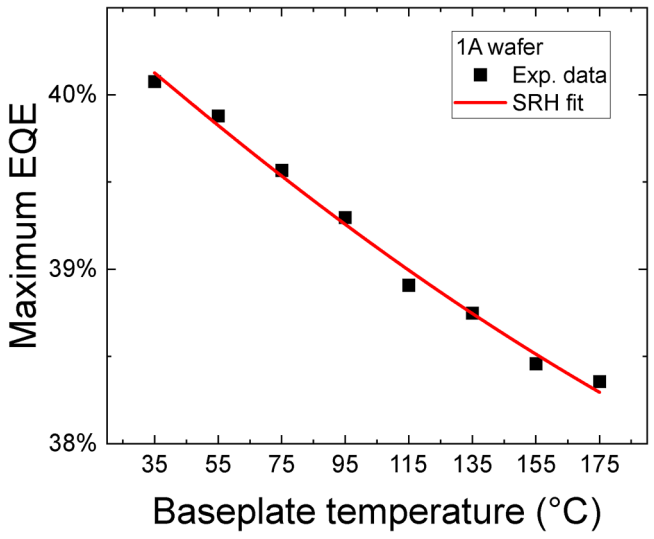

FIG. 5. External quantum efficiency maximum of the 1A sample with respect to the baseplate temperature (squares) and fitting with Eq. (2) (red line).

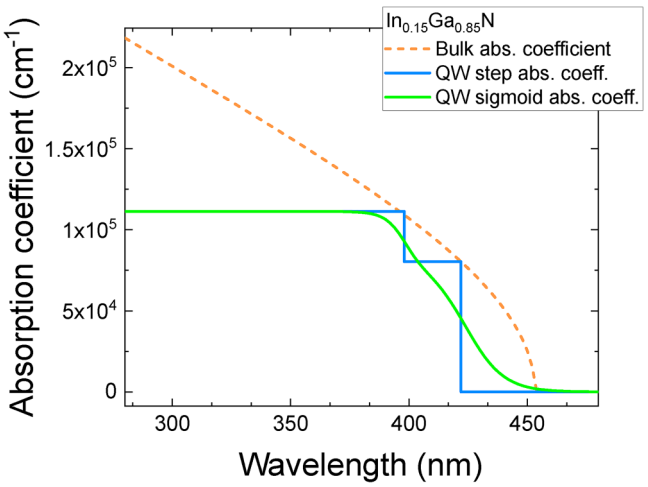

FIG. 6. InGaN bulk absorption coefficient (dashed orange curve), stepwise absorption coefficient for a two-level quantum system (blue solid curve), and smoothed absorption coefficient (green solid curve).

2. The light is absorbed according to the Lambert–Beer exponential absorption law,

$$I(x, E_{ph}, T) = I_0(E_{ph})e^{-\alpha(E_{ph},T)x}, \tag{3}$$

where x is the position, $I_0(E_{ph})$ is the light intensity entering the absorbing layer, and $\alpha(E_{ph})$ is the absorption coefficient. The last two terms depend on the photon energy, E_{ph}, related to the wavelength by the relation $E_{ph} = hc/\lambda$, where h is Planck's constant and c is the speed of light.

3. The absorption coefficient of the bulk GaN layers and MQW barrier layers has a square-root dependence on energy,[25]

$$\alpha(E_{ph}, T) = \alpha_0\sqrt{a(E_{ph} - E_g(T)) + b(E_{ph} - E_g(T))^2}, \tag{4}$$

where α_0, a, and b are material dependent coefficients and $E_g(T)$ is the material energy gap, whose temperature dependence is given by the Varshni law [see Eq. (1)].

4. MQW InGaN layers, on the other hand, have quantized energy levels due to quantum confinement.[26] Instead of using a sharp stepwise absorption coefficient, a more physical s-shaped sigmoid approximation that accounts for Urbach tail broadening is used,[27–29]

$$\alpha_{QW}(E_{ph}, T) = \frac{\alpha(E_g(T) + E_1)}{1 + \exp\left(\frac{E_g(T) + E_1 - E_{ph}}{\Delta E}\right)} + \sum_{n=2}^{m} \frac{\alpha(E_g(T) + E_n) - \alpha(E_g(T) + E_{n-1})}{1 + \exp\left(\frac{E_g(T) + E_n - E_{ph}}{\Delta E}\right)}, \tag{5}$$

where ΔE is an empirical term that accounts for the spreading of the sigmoid and $\alpha(E_g(T) + E_i)$ is the same as Eq. (4) evaluated for energies $E_g(T) + E_n$, where $E_n = E_n^e + E_n^h$ is the additional energy gap due to the quantization of the energy levels inside the quantum wells given as the sum of the nth energy level for electron and holes, respectively. Transitions with odd Δn are forbidden, whereas transitions for even Δn are allowed; however, it has been shown that in polarized $In_xGa_{1-x}N$–GaN quantum wells with $x < 0.2$, the transitions with $\Delta n = 0$ dominate, and, therefore, transitions with $\Delta n \neq 0$ with even Δn are ignored in this model.[30] The quantized energies of electrons and holes in the finite well can be calculated from the time-independent Schrodinger equation by considering that the potential at the bottom of the well is equal to $-V_0$ over a width of 3 nm,

$$-\frac{\partial^2\psi}{\partial x^2} - \frac{2m}{\hbar^2}V_0\psi = \frac{2m}{\hbar^2}E\psi. \tag{6}$$

In this approximation, piezoelectric field effects are ignored. An example of the absorption coefficient for a two-level quantum confined system is reported in Fig. 6.

5. Each absorbed photon produces an electron–hole pair that is extracted and generates an electrical current (i.e., the extraction efficiency η_{ext} is equal to 1), with no dependence on photon wavelength.

Thus, photons with energies between the InGaN energy gap and the GaN energy gap are absorbed only inside the quantum wells, whereas photons with energies above the GaN energy gap are absorbed by barrier GaN and bulk GaN also, as schematized in Fig. 7. For the quantum wells, a 600 meV bandgap discontinuity for the $In_{0.15}Ga_{0.85}n$/GaN structure can be estimated[14] with a 70:30

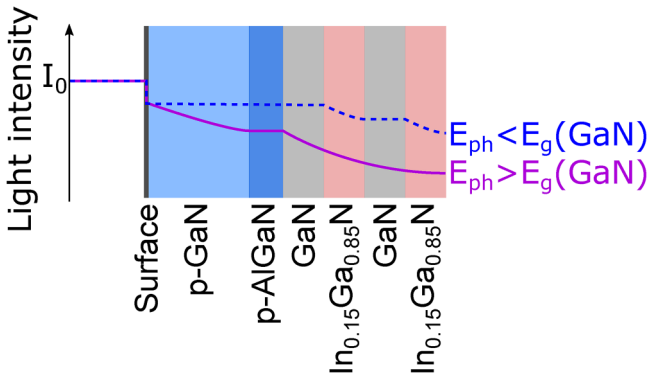

FIG. 7. Schematic of the light absorption model. A part of the light is reflected at the device surface. The remaining light is absorbed by InGaN layers only (if the photon energy is lower than the GaN energy gap) or by the GaN layer.

ratio between conduction and valence ratio discontinuity,[31] i.e., a well depth of 420 meV for electrons and 180 meV for holes. The time-independent Schrodinger equation was solved with effective mass $m_e^* = 0.18\ m_e$ and $m_h^* = 1.05\ m_e$, where m_e is the free electron mass. These effective masses for $In_{0.15}Ga_{0.85}N$ result from applying Vegard's law to InN and GaN bulk electron and hole effective masses.[32,33] Several energy levels sit inside the quantum wells with energies $E_1^e = 104$ meV, $E_2^e = 360$ meV for electrons, and $E_1^h = 23$ meV, $E_2^h = 90$ meV, and $E_3^h = 176$ meV with a corresponding $E_1 = E_1^e + E_1^h = 127$ meV and $E_2 = E_2^e + E_2^h = 450$ meV with the $\Delta n = 0$ selection rule. Therefore, summation in Eq. (5) is limited to $m = 2$.

To evaluate the photocurrent and the EQE of the device, we assumed that the carriers that are generated in the bulk p-GaN region are not collected. The physical reason of this assumption can be seen in the band diagram of Fig. 8. Since the bands in the p-GaN region are flate, diffusion, rather than drift, is involved in photogenerated carrier extraction. p-GaN thickness can be compared with the electron diffusion length in p-type GaN, which is around 200 nm, and could be even lower if we consider that p-GaN is heavily doped, therefore having a higher defect density and a higher SRH recombination ratio.[34] Moreover, the p-AlGaN layer also adds a 297 meV barrier for electrons, making their extraction more difficult when they are generated in the p-side of the device.[12]

The resulting photocurrent calculated with this model for the 1A sample, normalized with respect to the InGaN absorption peak (around 395 nm), is the green curve of Fig. 9(a), whereas the corresponding normalized EQE is shown in Fig. 9(b). Here, we show the normalized version of the photocurrent and EQE, respectively. It is worth noticing that the calculations were done by considering a unitary extraction efficiency and no losses due to recombination. Even under these assumptions, the spectral shape obtained experimentally was found to be accurately reproduced by the model. Photons with energy larger than the bandgap quickly thermalize to band edges (in the nanosecond or sub-nanosecond range[35,36]).

For GaN and InN, literature parameters for their absorption coefficients and for Varshni parameters were used. For $In_{0.15}Ga_{0.85}N$, Varshni-law parameters from experimental data

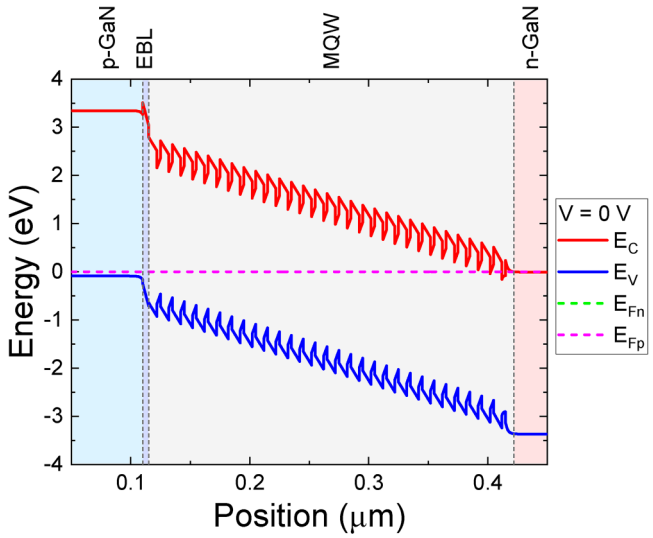

FIG. 8. Band diagram at 0 V for the 1A structure with a 100 nm p-GaN layer.

fitting were used, whereas the bulk absorption coefficient was calculated by using Eq. (4). The $In_{0.15}Ga_{0.85}N$ energy gap was evaluated from GaN and InN data through Vegard's law. If

$$E_g(In_xGa_{1-x}N) = x \times E_g(InN) + (1-x) \times E_g(GaN) - \beta \times x \times (1-x), \quad (7)$$

then Eq. (5) was used to calculate the quantum well absorption coefficient from the bulk InGaN absorption coefficient, as shown in Fig. 6. All the used parameters are reported in Table I.

However, there is a discrepancy between the experimental data and the model. The calculated edge of the GaN peak appears to be blue-shifted by about 20 nm, and, thus, the absorption in this region is somehow overestimated. Therefore, a second further hypothesis is considered, i.e., that the absorption edge of the bulk p-GaN has a lower energy than the usual value of 3.42 eV. This assumption makes physical sense if one considers that the p-GaN is heavily doped with magnesium. This generated shallow trap levels with energies in the range of 0.15– 0.20 eV. These levels generate an ultraviolet band on the gallium nitride with energies around 3.27 eV for donor–acceptor pair (DAP) transitions and around 3.1–3.2 eV for optical transitions from a conduction band to a shallow magnesium acceptor (e-A).[41,42] Considering these physical aspects results in a reduction in the quantum efficiency in the 360– 380 nm region; as a result, the modeled normalized curve now agrees with the experimental normalized curve (the blue curve in Fig. 9).

To prove the validity of the model, the EQE was also calculated for the 2A and 2B variants, which feature 50 and 150- nm p-GaN layers, respectively. Figure 10 reports the normalized external quantum efficiency: the secondary peak around 360 nm lowers with increasing p-GaN thickness. The model correctly describes the photocurrent behavior, thus confirming the validity of the

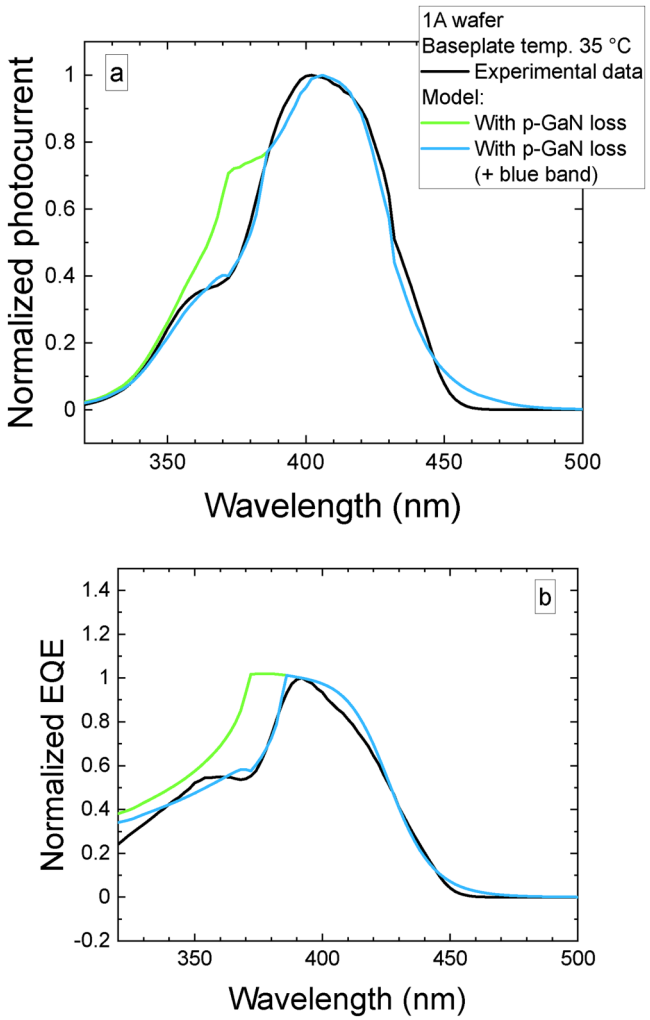

FIG. 9. Normalized photocurrent (a) and EQE (b) with respect to the value at 392 nm of the 1A wafer device: experimental data (black line), the model that considers the loss of the photogenerated carrier in p-GaN (green line), and the model that also considers the p-GaN absorption shift due to defects (blue line).

TABLE I. Coefficients used for model evaluation. The GaN and InN absorption coefficients are from Ref.37, and the GaN and InN Varshni coefficients are from Ref. 38. The InGaN absorption coefficient is from Eq. (9) in Ref. 37 evaluated for $x = 0.15$, the InGaN bowing parameter and $E_g(0)$ for InN and GaN are from Refs. 39 and 40, whereas the InGaN Varshni parameters are from experimental data fitting.

	$In_{0.15}Ga_{0.85}N$	GaN	InN
α_0 (cm^{-1})	10^5	10^5	10^5
a (eV^{-1})	1.556	3.525 17	0.696 42
b (eV^{-2})	−0.1182	−0.657 10	0.460 55
β	1.43	…	…
$E_g(0)$ (eV)	2.84	3.42	0.7
γ (eV/K)	6.6×10^{-4}	9.09×10^{-4}	2.45×10^{-4}
δ (K)	755	830	624

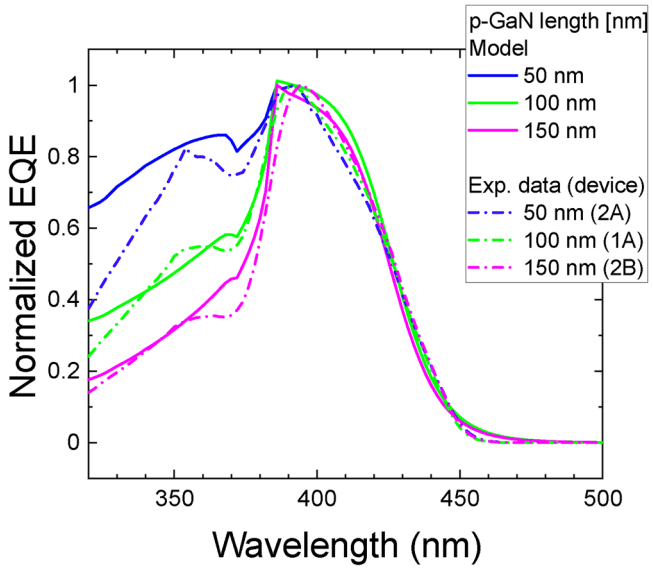

FIG. 10. Normalized EQE of 1A (green dashed-dotted line), 2A (purple dashed-dotted line), and 2B (blue dashed-dotted line) wafer device, and photocurrent calculated by the model for 50 (blue solid line), 100 (green solid line), and 150 nm (purple solid line).

previously made assumptions on the loss of the photogenerated carriers in the p-GaN layer.

Finally, the behavior of the EQE by varying the temperature was studied, and the normalized value to the one at 35 °C is shown in Fig. 11. From this figure, it is possible to see that the edge shift

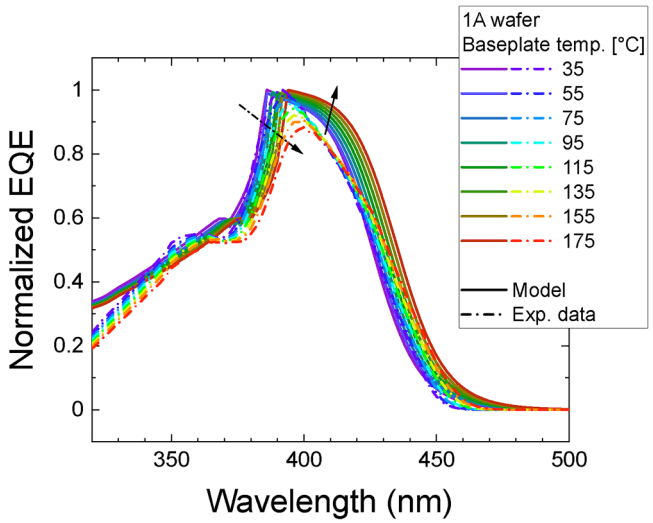

FIG. 11. Experimental values (dashed-dotted lines) and calculated values (solid lines) of the EQE, normalized by the value at 35 °C, of the 1A wafer at various baseplate temperatures.

due to the Varshni law is well predicted by the model. However, while the photocurrent is constant or slightly decreases with increasing temperature, the photocurrent predicted by the model increases with increasing temperature. This is due to the fact that the increasing temperature results in a shift of the absorption edge toward a region in which the light intensity supplied by the source is higher. It is worth mentioning that the current version of the model does not take into account the increase in SRH recombination that lowers the extraction efficiency from the quantum wells, thus compensating the higher absorption due to the energy gap shift.

CONCLUSIONS

In conclusion, we studied the quantum efficiency of InGaN–GaN multiple quantum well solar cells with a AlGaN electron-blocking layer and different p-GaN layer thicknesses under different light intensities and temperatures. We developed a model, based on simple assumptions, that allowed to calculate the generated photocurrent by taking into account the thicknesses of the various layers. We proved that the model can well reproduce the photocurrent characteristics of the cells. In addition, we found that p-GaN layer thickness has an influence on the quantum efficiency for wavelengths below 380 nm since the carriers photogenerated in this region cannot be efficiently collected. Moreover, the heavy magnesium doping of the p-GaN layer causes a redshift in the GaN absorption edge. The model successfully predicts the shape of the EQE of devices with different p-GaN layer thicknesses and its behavior at different temperatures.

SUPPLEMENTARY MATERIAL

See the supplementary material for the device reflectivity data and the EQE at different temperatures and different intensities of the 2A and 2B samples.

ACKNOWLEDGMENTS

The work at the University of Padova was partly performed within the project INTERNET OF THINGS: SVILUPPI METODOLOGICI, TECNOLOGICI E APPLICATIVI, co-founded (2018–2022) by the Italian Ministry of Education, Universities and Research (MIUR) under the aegis of the "Fondo per il finanziamento dei dipartimenti universitari di eccellenza" initiative (Law 232/2016). The work at Arizona State University and Rice University was partially supported by ULTRA, an Energy Frontier Research Center (EFRC) funded by the U.S. Department of Energy, Office of Science, Basic Energy Sciences under Award No. DE-SC0021230.

AUTHOR DECLARATIONS

Conflict of Interest

The authors have no conflicts to disclose.

DATA AVAILABILITY

The data that support the findings of this study are available within the article and its supplementary material.

REFERENCES

[1]See https://www.nrel.gov/pv/cell-efficiency.html for "NREL Research Cell Record Efficiency Chart;" accessed 10 January 2022.
[2]L. A. Reichertz, I. Gherasoiu, K. M. Yu, V. M. Kao, W. Walukiewicz, and J. W. Ager, "Demonstration of a III–nitride/silicon tandem solar cell," Appl. Phys. Express **2**, 122202 (2009).
[3]N. Laxmi, S. Routray, and K. P. Pradhan, "III–nitride/Si tandem solar cell for high spectral response: Key attributes of auto-tunneling mechanisms," Silicon **12**, 2455–2463 (2020).
[4]G. Moses, X. Huang, Y. Zhao, M. Auf der Maur, E. A. Katz, and J. M. Gordon, "InGaN/GaN multi-quantum-well solar cells under high solar concentration and elevated temperatures for hybrid solar thermal-photovoltaic power plants," Prog. Photovolt. Res. Appl. **28**, 1167 (2020).
[5]R. Dahal, J. Li, K. Aryal, J. Y. Lin, and H. X. Jiang, "InGaN/GaN multiple quantum well concentrator solar cells," Appl. Phys. Lett. **97**, 073115 (2010).
[6]X. Zheng, D. Zhang, X. Li, Y. Wu, H. Wang, X. Gan, N. Wang, and H. Yang, "InGaN-based multiple quantum well photovoltaic cells with good open-circuit voltage and concentration behavior," in *Proceedings of the 2013 IEEE 39th Photovoltaic Specialists Conference (PVSC)* (IEEE, 2013), pp. 2154–2156.
[7]D.-H. Lien, Y.-H. Hsiao, S.-G. Yang, M.-L. Tsai, T.-C. Wei, S.-C. Lee, and J.-H. He, "Harsh photovoltaics using InGaN/GaN multiple quantum well schemes," Nano Energy **11**, 104–109 (2015).
[8]C. De Santi, M. Meneghini, A. Caria, E. Dogmus, M. Zegaoui, F. Medjdoub, B. Kalinic, T. Cesca, G. Meneghesso, and E. Zanoni, "GaN-based laser wireless power transfer system," Materials **11**, 153 (2018).
[9]Y. Zhao, X. Huang, H. Fu, H. Chen, Z. Lu, J. Montes, and I. Baranowski, "InGaN-based solar cells for space applications," in *Midwest Symposium on Circuits and Systems* (IEEE, *2017*), pp. 954–957.
[10]R. Dahal, B. Pantha, J. Li, J. Y. Lin, and H. X. Jiang, "InGaN/GaN multiple quantum well solar cells with long operating wavelengths," Appl. Phys. Lett. **94**, 063505 (2009).
[11]J.-K. Sheu, F.-B. Chen, S.-H. Wu, M.-L. Lee, P.-C. Chen, and Y.-H. Yeh, "Vertical InGaN-based green-band solar cells operating under high solar concentration up to 300 suns," Opt. Express **22**, A1222 (2014).
[12]X. Huang, H. Chen, H. Fu, I. Baranowski, J. Montes, T. H. Yang, K. Fu, B. P. Gunning, D. D. Koleske, and Y. Zhao, "Energy band engineering of InGaN/GaN multi-quantum-well solar cells via AlGaN electron- and hole-blocking layers," Appl. Phys. Lett. **113**, 043501 (2018).
[13]A. Caria, C. De Santi, E. Dogmus, F. Medjdoub, E. Zanoni, G. Meneghesso, and M. Meneghini, "Excitation intensity and temperature-dependent performance of InGaN/GaN multiple quantum wells photodetectors," Electronics **9**, 1840 (2020).
[14]P. G. Moses and C. G. Van de Walle, "Band bowing and band alignment in InGaN alloys," Appl. Phys. Lett. **96**, 021908 (2010).
[15]J. R. Lang, N. G. Young, R. M. Farrell, Y.-R. Wu, and J. S. Speck, "Carrier escape mechanism dependence on barrier thickness and temperature in InGaN quantum well solar cells," Appl. Phys. Lett. **101**, 181105 (2012).
[16]W. Shockley and W. T. Read, "Statistics of the recombinations of holes and electrons," Phys. Rev. **87**, 835–842 (1952).
[17]M. Meneghini, C. De Santi, I. Abid, M. Buffolo, M. Cioni, R. A. Khadar, L. Nela, N. Zagni, A. Chini, F. Medjdoub *et al.*, "GaN-based power devices: Physics, reliability, and perspectives," J. Appl. Phys. **130**, 181101 (2021).
[18]A. Armstrong, A. R. Arehart, B. Moran, S. P. DenBaars, U. K. Mishra, J. S. Speck, and S. A. Ringel, "Impact of carbon on trap states in n-type GaN grown by metalorganic chemical vapor deposition," Appl. Phys. Lett. **84**, 374 (2004).
[19]A. R. Arehart, T. Homan, M. H. Wong, C. Poblenz, J. S. Speck, and S. A. Ringel, "Impact of N- and Ga-face polarity on the incorporation of deep levels in n -type GaN grown by molecular beam epitaxy," Appl. Phys. Lett. **96**, 242112 (2010).
[20]A. R. Arehart, A. Corrion, C. Poblenz, J. S. Speck, U. K. Mishra, S. P. DenBaars, and S. A. Ringel, "Comparison of deep level incorporation in

ammonia and rf-plasma assisted molecular beam epitaxy n-GaN films," Phys. Status Solidi C **5**, 1750–1752 (2008).
[21]Y. Nakano, "Deep-level defects in homoepitaxial p-type GaN," J. Vac. Sci. Technol. A **36**, 023001 (2018).
[22]C. E. Dreyer, A. Alkauskas, J. L. Lyons, J. S. Speck, and C. G. Van De Walle, "Gallium vacancy complexes as a cause of Shockley-Read-Hall recombination in III-nitride light emitters," Appl. Phys. Lett. **108**, 141101 (2016).
[23]J. L. Lyons and C. G. Van De Walle, "Computationally predicted energies and properties of defects in GaN," npj Comput. Mater. **3**, 1–10 (2017).
[24]M. A. Reshchikov, D. O. Demchenko, A. Usikov, H. Helava, and Y. Makarov, "Carbon defects as sources of the green and yellow luminescence bands in undoped GaN," Phys. Rev. B **90**, 235203 (2014).
[25]G. F. Brown, J. W. Ager, W. Walukiewicz, and J. Wu, "Finite element simulations of compositionally graded InGaN solar cells," Sol. Energy Mater. Sol. Cells **94**, 478–483 (2010).
[26]M. Fox and M. Anthony, *Optical Properties of Solids* (Oxford University Press, 2010), p. 396.
[27]F. Urbach, "The long-wavelength edge of photographic sensitivity and of the electronic absorption of solids," Phys. Rev. **92**, 1324 (1953).
[28]K. P. O'Donnell, R. W. Martin, and P. G. Middleton, "Origin of luminescence from InGaN diodes," Phys. Rev. Lett. **82**, 237 (1999).
[29]B. Damilano, N. Grandjean, J. Massies, L. Siozade, and J. Leymarie, "InGaN/GaN quantum wells grown by molecular-beam epitaxy emitting from blue to red at 300 K," Appl. Phys. Lett. **77**, 1268 (2000).
[30]C. Wetzel, S. Kamiyama, H. Amano, and I. Akasaki, "Optical absorption in polarized $Ga_{1-x}In_xN$/GaN quantum wells," Jpn. J. Appl. Phys. **41**, 11 (2002).
[31]G. Martin, A. Botchkarev, A. Rockett, and H. Morkoç, "Valence-band discontinuities of wurtzite GaN, AlN, and InN heterojunctions measured by x-ray photoemission spectroscopy," Appl. Phys. Lett. **68**, 2541–2543 (1996).
[32]U. M. E. Christmas, A. D. Andreev, and D. A. Faux, "Calculation of electric field and optical transitions in InGaN/GaN quantum wells," J. Appl. Phys. **98**, 073522 (2005).
[33]A. Gorai, S. Panda, and D. Biswas, "Advantages of InGaN/InGaN quantum well light emitting diodes: Better electron-hole overlap and stable output," Optik **140**, 665–672 (2017).
[34]Z. Z. Bandić, P. M. Bridger, E. C. Piquette, and T. C. McGill, "Electron diffusion length and lifetime in p-type GaN," Appl. Phys. Lett. **73**, 3276 (1998).
[35]X. Zhang, D. H. Rich, J. T. Kobayashi, N. P. Kobayashi, and P. D. Dapkus, "Carrier relaxation and recombination in an InGaN/GaN quantum well probed with time-resolved cathodoluminescence," Appl. Phys. Lett. **73**, 1430 (1998).
[36]Y. Zhang, G. Conibeer, S. Liu, J. Zhang, and J. F. Guillemoles, "Review of the mechanisms for the phonon bottleneck effect in III–V semiconductors and their application for efficient hot carrier solar cells," Prog. Photovolt. Res. Appl. **30**, 581 (2022).
[37]R. Belghouthi, S. Taamalli, F. Echouchene, H. Mejri, and H. Belmabrouk, "Modeling of polarization charge in N-face InGaN/GaN MQW solar cells," Mater. Sci. Semicond. Process. **40**, 424–428 (2015).
[38]S. C. Jain, M. Willander, J. Narayan, and R. V. Overstraeten, "III–nitrides growth, characterization, and properties," J. Appl. Phys. **87**, 965–1006 (2000).
[39]J. Wu, W. Walukiewicz, K. M. Yu, J. W. Ager III, E. E. Haller, H. Lu, and W. J. Schaff, "Small band gap bowing in $In_{1-x}Ga_xN$ alloys," Appl. Phys. Lett. **80**, 4741 (2002).
[40]J. Wu and W. Walukiewicz, "Band gaps of InN and group III nitride alloys," Superlattices Microstruct. **34**, 63–75 (2003).
[41]M. A. Reshchikov, G.-C. Yi, and B. W. Wessels, "Behavior of 2.8- and 3.2-eV photoluminescence bands in Mg-doped GaN at different temperatures and excitation densities," Phys. Rev. B **59**, 13176 (1999).
[42]M. A. Reshchikov and H. Morkoç, "Luminescence from defects in GaN," Phys. B Condens. Matter **376–377**, 428–431 (2006).